

# Personalized Ventricular Arrhythmia Simulation Framework to Study Vulnerable Trigger Locations on Top of Scar Substrate

Kevin D Lau<sup>1</sup>, Alexandra Groth<sup>2</sup>, Irina Waechter-Stehle<sup>2</sup>, Uyen Chau Nguyen<sup>3</sup>, Paul GA Volders<sup>3</sup>, Jordi Heijman<sup>3</sup>, Jürgen Weese<sup>2</sup>, Matthijs JM Cluitmans<sup>1,3</sup>

<sup>1</sup>Philips Research, Eindhoven, the Netherlands

<sup>2</sup>Philips Research, Hamburg, Germany

<sup>3</sup>CARIM, Maastricht University Medical Centre, Maastricht, the Netherlands

## Abstract

*Personalized arrhythmia simulations have the potential to improve diagnosis and guide therapy. Here, we introduce a computational framework for personalized simulations of ventricular electrophysiology (EP) incorporating scar. This framework was utilized to study arrhythmia mechanisms in a patient who had a sudden cardiac arrest due to ventricular fibrillation (VF).*

*From delayed enhancement magnetic resonance imaging (MRI) an anatomical model was constructed by deforming a generic model to the image. Regions of scar and border zone were segmented by thresholding. EP was then simulated using the CARPentry monodomain solver. The Ten Tusscher ventricular EP model was adapted locally to reflect healthy, border zone or scar tissue. In this patient, three distinct premature ventricular complexes (PVCs) were identified using electrocardiographic imaging (ECGI), one of which induced VF. The clinically observed PVCs were then replicated in the virtual model to study arrhythmia development, but VF could not be reproduced with a simple stimulation protocol that disregarded patient-specific conditions present at the time of actual VF induction. This could indicate that not only the virtual heart model, but also the stress test may need to be personalized for accurate arrhythmia simulations.*

*In conclusion, this computational framework enables EP simulations based on MRI-detected scar and triggers, and allows to study the amount of personalization required for accurate EP simulations.*

## 1. Introduction

After decades of academic developments, personalized biophysical simulation is reaching clinical application in the field of cardiovascular medicine.[1] One promising

field is that of personalized arrhythmia simulation, which may help to predict the need for therapy after myocardial infarction (MI) through implantable devices or invasive ablation therapy.[2], [3] This typically requires image data (such as magnetic resonance imaging, MRI) to detect an individual's substrate for arrhythmias, and personalizing an electrophysiology (EP) model with these data to test the arrhythmic characteristics of this substrate. However, the frameworks to perform these personalized simulations are currently very time consuming and labour intensive, making them impractical for routine clinical application. To release the true clinical potential of these approaches, there is a need for a stable, practically applicable pipeline. This also allows studying the amount of personalization required for accurate arrhythmia simulations.

## 2. Pipeline

Elements of an image-based personalized EP simulation pipeline include: 1) Image segmentation, i.e., to delineate the cardiac structures from an MRI scan, with a separation of healthy tissue and diseased tissue; 2) Generating a computational mesh from those segmentations; 3) Personalizing the electrophysiological properties of that mesh; and 4) Performing personalized simulations to study arrhythmia mechanisms. Our implementation of these elements is described in this paper.

## 3. Image segmentation

Our previously described model-based segmentation adapts a 'general' mesh model of the organ to an image. This general heart is represented as a triangulated mesh with a fixed number of vertices and triangles. A generalized Hough transformation is used to place the general heart mesh in the patient's image. Next, a parametric and deformable adaptation is performed using

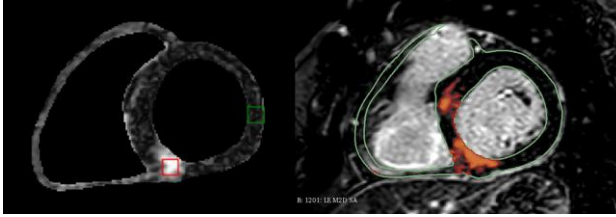


Figure 1. Left: Regions used for sampling scar (red box) and healthy myocardial (green box) signal intensity. Right: Segmentation of scar (light red) and border zone (dark red) by thresholding.

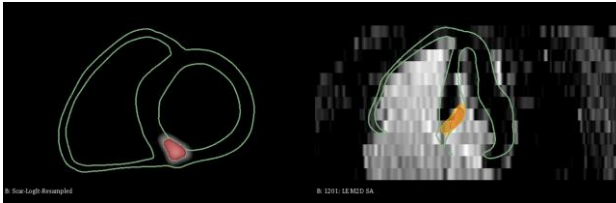


Figure 2. Left: Conversion of the scar mask to the LogIt function (white) and thresholding of the scar region (red). Right: Visualisation of the scar/border interpolation out-of-plane.

triangle-specific boundary detectors to further tune the mesh to the image. [4]

This approach has been adapted for the simulation framework. In particular, the heart mesh was modified to include both epi- and endocardial walls for the left and the right ventricle. In addition, boundary detectors have been trained on cine MR images to enable automatic adaptation of the model to images. For boundary detection training a recently proposed approach using neural networks and deep learning was used. [5] The resulting prototype was used to generate an automatic segmentation of left/right ventricles/atria. This segmentation was manually adjusted to correctly account for the scar and border regions that were incorrectly interpreted as blood pool.

Scar and border-zone regions were segmented using the threshold based approach detailed by Schmidt et al [6]. Following this approach, representative regions identified to determine maximum signal intensities for scar and healthy myocardium (Figure 1). The scar was defined as voxels with intensities ranging from 50% to 100% of the maximum signal intensity (SI) of the scar region. Similarly, the border zone was defined as the voxels ranging from the maximum SI of the myocardial region to 50% of the maximum SI of the scar region. Here only voxels within the LV and RV boundaries were thresholded. Lone thresholded voxels not connected to continuous regions were manually removed.

The 3D geometry of the scar/border zone was then reconstructed using the approach detailed by Ukwatta et al. [7]: On each axial slice the scar/border zone mask was converted using the LogIt function and then interpolated in

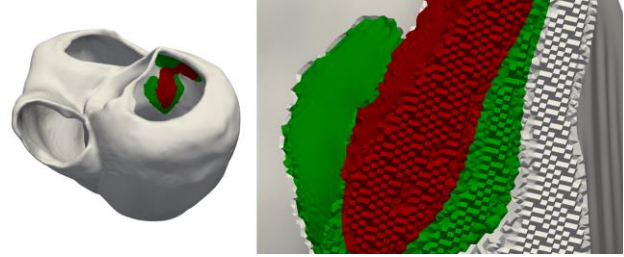


Figure 3. Left: Computational mesh, with healthy myocardium in grey, border zone in green and scar in red. Right: Cut view showing the mesh consisting of tetrahedral, pyramids and hexahedral elements.

the coronal and sagittal directions using an isotropic voxel sizing of 0.5 mm (Figure 2).

#### 4. Computational mesh

A volumetric computational mesh was created from the thresholded and interpolated surfaces meshes of the healthy myocardium, border zone and scar regions. A hybrid meshing approach was adopted in which a mixed mesh consisting of tetrahedral, pyramid and hexahedral elements was created (Figure 3). Specifically, the Octree mesh generator from ANSYS ICEM was used to create a mesh with tetrahedral elements at the interface between different tissue regions and hexahedral elements in regions far from these interfaces. The sizing parameters were modified until the average edge length throughout the whole mesh was 0.5 mm.

#### 5. Electrophysiology simulations

The electrophysiology properties of this virtual heart were studied with simulations based on the monodomain formulation as implemented in CARPentry (<https://carpentry.medunigraz.at/carputils/index.html>). In the healthy myocardium the ten Tusher ionic model was used [8]. In the border zone this ionic model was modified by reducing the ion channel current conduction. Here the following percentage reductions were adopted following Arevalo et al. [2]: GNa -62%, GCaL -69%, Gkr -70% and GK1 -80%. Next, the cardiac fibre orientation was generated using the rule based approach as detailed by Bayer et al. [9] (Figure 4).

The conductivity parameters in the monodomain equations were initialized by matching a conduction velocity of 0.6 and 0.3 m/s in the fibre and transverse directions, respectively, of a pseudo-1D cable model. This cable model only consisted of hexahedral elements; other numerical parameters (e.g., time integrator, time step size and ionic model) were identical to the whole heart model. Following Arevalo et al. [2] the transverse conductivity in

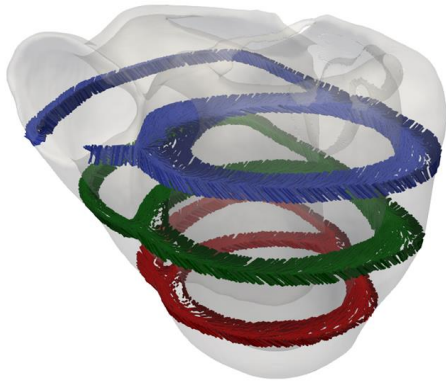


Figure 4. Visualisation of the fibre orientation in different planes.

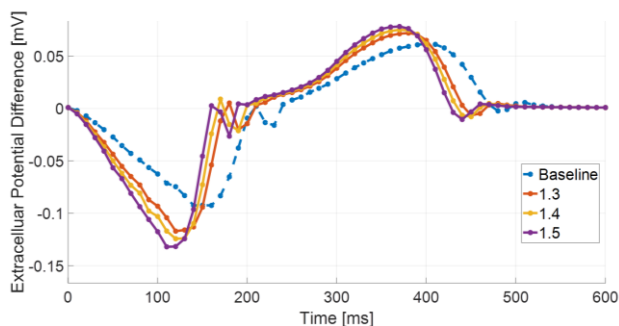


Figure 5. Pseudo-ECG resulting from the baseline conductivity values (tuned to a cable), and pseudo-ECGs resulting from increased conductivities (to 130, 140 and 150% of cable-tuned conductivity) to arrive at realistic QRS width.

the border zone scaled to 90% of the healthy value. Whole heart electrophysiology simulations were then performed from a single stimulus location. From those, a pseudo-ECG was reconstructed from the extracellular potential difference between two locations (apical vs basal), Figure 5. The conductivity values were then scaled until the QRS duration was approximately 180 ms to match typical literature values for premature beats [10].

## 6. Personalized simulations

This pipeline was executed in one patient case. This male patient of 40 years had myocardial scar after previous radiotherapy, with paroxysmal atrial fibrillation (AF). MRI revealed the presence of scar tissue. During an isoprenaline provocation test, the subject developed frequent premature ventricular complexes (PVCs) of three different types. Whereas the first two types occurred frequently without any consequence, the single occurrence of the third type directly resulted in ventricular fibrillation (VF), which

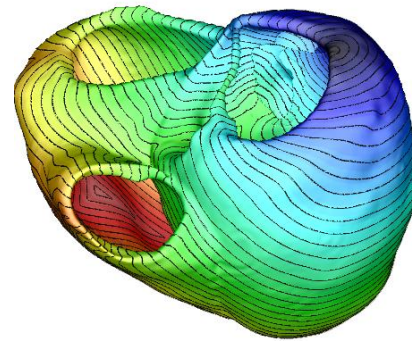


Figure 6. Activation time isochrones (with 5 ms contours) for a simulated beat in the personalized geometry.

required electrical cardioversion. During the provocation test, electrocardiographic imaging [11] was performed to determine the origin of the three distinct PVCs. The personalized virtual heart model was then triggered from the same three locations to study whether it was possible to replicate the clinical observation. The trigger protocol followed the stimulation protocol described by Arevalo et al. [2] In short, for each of the three locations a baseline pacing with 600 ms cycle length (CL) was followed by an extra stimulus with decreasing CL until no capture was possible anymore. If no arrhythmia was induced, the shortest CL with capture was followed by another series of stimuli with decreasing CL until an arrhythmia developed or a maximum train of four extra stimuli was reached.

For the two PVC locations that did not show a VF induction in the patient, it was impossible to induce an arrhythmia in the simulation. Interestingly, also for the PVC that clinically induced an arrhythmia, the virtual heart was not inducible (Figure 6). This may be caused by several factors:

- The baseline pacing of the virtual heart model was based on single-location stimuli, while the patient's baseline ventricular rhythm was conducted through the heart's conduction system ensuring a quick, homogeneous activation and recovery of the ventricles. The recovery substrate may therefore be quite different between the patient's actual and virtual baseline rhythm.
- The localization of the PVC origins was executed through ECGI, which is known to have a 1-2 cm inaccuracy. [11] Additionally, our implementation of ECGI does not differentiate between epicardial or septal origins. This locational variability may play an important role in the trigger-substrate relationship.
- The episode of VF occurred during AF and isoprenaline provocation; both conditions are

currently not included in the virtual heart model.

All these elements require further personalization of the stress test, and may be essential to arrive at truly personal arrhythmia understanding. An easy-to-apply framework as described here provides an essential basis for such understanding.

## 7. Discussion

In this study, we have introduced the first steps towards a robust and clinically applicable EP modelling framework that can be personalized by incorporating MRI-detected substrate to study its arrhythmogenic consequence. This personalized framework allows to study the interaction between triggers and substrate in a controlled environment. It highlights the potential need for further personalization to obtain a more thorough, patient-specific understanding of arrhythmia mechanisms leading to sudden life-threatening arrhythmias such as VF.

It remains an open question what amount of personalization is required for these models. We have employed the common approach here, which includes only personalizing the distribution of scar, border zone and healthy tissue. The EP characteristics of these regions such as ion channel distribution and tissue conductivity are based on (averaged) cohort data. Similarly, the fibre orientation is not personalized but based on a rule-based approach. Consequently, one may also wonder how complex these personalized simulations need be for accurate arrhythmia simulations. The ten Tusscher model employed in this study is relatively complex and computationally demanding, whereas EP characteristics of the different regions are based on limited data and not personalized. A simpler ionic model may capture similar AP changes with less computational effort, but it should be studied whether this would still provide similar accuracy at an individual level.

Additionally, the cardiac mesh is build from 10mm-thick MRI slices which may miss essential parts of a re-entry circuit such as microchannels. Isovolumetric 3D MRI with submillimetre level may provide more insight in the scar distribution, but this technique is currently not widespread available in a clinical setting.

More over, next to model personalization also the stress test may be further personalized by including the heart's conduction system, by including drug testing, by including comorbidities such as AF, and by investigating a larger range of trigger locations.

In conclusion, we have demonstrated the first steps towards a practically applicable computational framework for personalized EP simulations, illustrated with a patient case. Open questions remain on the level of detail and personalization required to capture the full complexity of arrhythmogenesis and should be tuned to the relevant clinical goal. The semi-automatic pipeline introduced in this paper sets the stage to study these questions in a robust

manner that allows future extension to clinical application.

## Conflicts of interest

None.

## References

- [1] M. A. Hlatky *et al.*, "Quality-of-Life and Economic Outcomes of Assessing Fractional Flow Reserve with Computed Tomography Angiography: PLATFORM," *J. Am. Coll. Cardiol.*, vol. 66, no. 21, pp. 2315–2323, 2015.
- [2] H. J. Arevalo *et al.*, "Arrhythmia risk stratification of patients after myocardial infarction using personalized heart models," *Nat. Commun.*, vol. 7, p. 11437, May 2016.
- [3] A. Prakosa *et al.*, "Personalized virtual-heart technology for guiding the ablation of infarct-related ventricular tachycardia," *Nat. Biomed. Eng.*, Sep. 2018.
- [4] O. Ecabert *et al.*, "Segmentation of the heart and great vessels in CT images using a model-based adaptation framework," *Med. Image Anal.*, vol. 15, no. 6, pp. 863–76, Dec. 2011.
- [5] T. Brosch, J. Peters, A. Groth, T. Stehle, and J. Weese, "Deep Learning-Based Boundary Detection for Model-Based Segmentation with Application to MR Prostate Segmentation," 2018, pp. 515–522.
- [6] A. Schmidt *et al.*, "Infarct tissue heterogeneity by magnetic resonance imaging identifies enhanced cardiac arrhythmia susceptibility in patients with left ventricular dysfunction," *Circulation*, vol. 115, no. 15, pp. 2006–2014, 2007.
- [7] E. Ukwatta *et al.*, "Image-based reconstruction of three-dimensional myocardial infarct geometry for patient-specific modeling of cardiac electrophysiology," *Med. Phys.*, vol. 42, no. 8, pp. 4579–4590, 2015.
- [8] K. H. W. J. ten Tusscher and A. V. Panfilov, "Alternans and spiral breakup in a human ventricular tissue model," *Am. J. Physiol. Circ. Physiol.*, vol. 291, no. 3, pp. H1088–H1100, Sep. 2006.
- [9] J. D. Bayer, R. C. Blake, G. Plank, and N. A. Trayanova, "A novel rule-based algorithm for assigning myocardial fiber orientation to computational heart models," *Ann. Biomed. Eng.*, vol. 40, no. 10, pp. 2243–2254, 2012.
- [10] K. P. Moulton, T. Medcalf, and R. Lazzara, "Premature ventricular complex morphology: A marker for left ventricular structure and function," *Circulation*, vol. 81, no. 4, pp. 1245–1251, 1990.
- [11] M. J. M. Cluitmans *et al.*, "In Vivo Validation of Electrocardiographic Imaging," *JACC Clin. Electrophysiol.*, vol. 3, no. 3, 2017.

Address for correspondence: MJM Cluitmans, CARIM, Maastricht University, P.O. Box 616, 6200MD Maastricht, The Netherlands, m.cluitmans@maastrichtuniversity.nl.